Supplementary Materials

2. Materials and methods

2.1. Materials

Food grade deacetylated gellan (KELCOGEL) was obtained from CP Kelco (Chicago, US). Hydroxypropyl methylcellulose (HPMC) and poly-ε-caprolactone (PCL) were obtained from Sigma Aldrich (USA). Disodium hydrogen phosphate, potassium dihydrogen phosphate potassium chloride, and calcium chloride were purchased from Qualigen Fine Chemicals (India). 1,2-dioleoyl-sn-glycero-3-phosphoethanolamine (DOPE) and hexadecyl phosphocholine (HePc) or miltefosine (purity >99%) were obtained from Avanti Polar Lipids (Alabaster, AL, USA) and Lipoid GmbH (Germany) respectively. Temozolomide (TMZ) of >99% purity was obtained from Ark Pharma. Inc. (China). Soya phosphatidylcholine (SPC), N-hydroxysuccinimide (NHS), 1-ethyl-3-[3-dimethylaminopropyl] carbodiimide (EDC), and 3(4,5-dimethyl- thiazol-2-yl)-2,5-diphenyl-tetrazolium bromide (MTT) were obtained from HiMedia Laboratories Pvt Ltd. (India). Human holo-transferrin with purity >99% was purchased from Sigma Aldrich, (India). Fluorescein isothiocyanate (FITC), rhodamine-6G, and Nile red were procured from Anaspec Inc. (USA). The Ki67 and Caspase-3 antibodies were procured from GeneTex, India. The bicinchoninic acid protein assay kit (BCA),2-(N-morpholino) ethanesulfonic acid (MES), and high-pressure liquid chromatography (HPLC) grade acetonitrile, chloroform, and methanol were purchased from Thermo Scientific (USA) and Merck (India) respectively. Milli-Q water with 18.2MΩcm resistivity was used in all studies using the Millipore (USA) system.

2.2. Nanovesicle generation

Nanovesicles without TMZ were prepared by modified thin-film hydration technique. Briefly, the mixture of previously optimized ratios [17] of phospholipids (60-90mol % of SPC, 10-40mol% of HePc, 1mg of DOPE) was dissolved in a 1:2v/v mixture of methanol and chloroform in a round bottom flask (RBF). Slow evaporation of organic solvent using rotary vacuum evaporator at 40^{O}C for 45min at 150rpm leading to the formation of thin lipid film. Subsequently, thin film was hydrated at 45^{O}C for 1hr at 120rpm in phosphate-buffered saline (pH 7.4). Branson Sonifier 450 probe sonicator was used to sonicate the suspension at 50% amplitude and 20kHz for 2min followed by centrifugation for 45min under 4^{O}C at 25,000g. The pelleted nanovesicles was resuspended in phosphate buffer saline and were labeled as non-

targeted nanovesicles (LNs) depending on the preselected molar ratio of HePc to soya PC. Similarly, rhodamine-6G (excitation wavelength: 400-570nm; emission wavelength: 500-650nm) labeled nanovesicles was prepared. Temozolomide (TMZ) loaded non-targeted nanovesicles (LNs-TMZ), was prepared by a similar procedure used for blank nanovesicles described above, with slight modification i.e. incorporation of a drug in hydration step to load it in the aqueous phase of the nanovesicles. The TMZ loaded non-targeted nanovesicles were labeled as LNs-TMZ.

Transferrin (Tf) targeted nanovesicles (TLNs) were prepared by covalent linking of Tf to nanovesicles as per our previously optimized protocol [15]. Finally, targeted nanovesicles with and without TMZ were labeled as Tf-LNs and Tf-LNs-TMZ, respectively.

2.3. Nanovesicle characterizations

Nanovesicle hydrodynamic size, polydispersity index, and zeta potential were characterized by photon correlation spectroscopy using laser particle analyzer (BI200SM, Brookhaven Instrument Corporation, USA) and ZetaPALS, Brookhaven Instrument Corporation, (USA) respectively. TMZ encapsulation in targeted/non-targeted nanovesicles was quantified by high-resolution liquid chromatography-mass spectroscopy method (model 1290 UHPLC infinity system, connected with Jet Stream ESI source, 6550iFunnel Q-TOF, and C18 column {ZORBAX SB-C18 rapid resolution HD 2.1X50mm, 1.8µm} of Agilent Technologies {USA}) following previously reported method [16]. A high-resolution transmission electron microscope (HR-TEM, model JEM 2100 ultra) was used to evaluate the morphology of the nanovesicles. The combination index (CI) of TMZ and HePc was quantified using the classic iso-bologram method to find out whether the combination was additive, synergistic, or antagonist as per the previously described method [17-19].

We then measured the phospholipid (PL) concentration following a similar protocol reported using UV-Visible spectroscopy at 485nm [20]. Whereas, the mean amount of Tf conjugated to nanovesicles in terms of the number of phospholipids was quantified by bicinchoninic acid (BCA) protein assay kit [21]. Flow cytometry (BD FACScalibur, USA) analysis was carried out to determine the conjugation between nanovesicles and Tf. Briefly, fluorescein isothiocyanate (FITC) tagged Tf was applied to identify the conjugation between nanovesicles and protein. The nanovesicles were labeled with Nile red. The excitation and emission spectra of Nile red is 553nm and 636nm respectively, while, the excitation and emission spectra of FITC is 495nm and 525nm respectively). The unstained conjugated nanovesicles was used as

control. Test sample composed of conjugated nanovesicles labeled with both the dyes (i.e. Nile red plus FITC). Additionally, two compensation controls we used in our study i.e. compensation control 1 of conjugated nanovesicles labeled with Nile red, and compensation control 2 of conjugated nanovesicles labeled with FITC.

2.4. Preparation of biopolymeric hydrogels

Biopolymeric hydrogels were prepared by dissolving GG (0.6%w/v) and HPMC (0.4%w/v, 0.3%w/v and 0.2%w/v) to a final concentration of 1%, 0.9% and 0.8% w/v respectively to the total polymer weight of 1%w/v at 1500rpm for 24h. At the end of 24h, tween-80 (1%v/v) was mixed to the above hydrophilic polymer solution. Subsequently, PCL (0.1%w/v, 0.2%w/v and 0.3%w/v in dichloromethane) was added dropwise (1ml/min) to form an emulsion. The reaction was continued for another 24h resulting in the formation of a stable emulsion-based polymer blend. Finally, the *in-situ* hydrogels were formed by heating the aforementioned emulsion blend at 42±1^{O}C at 1500rpm. The final concentration of GG: HPMC: PCL were 0.6:0.4:0.0%w/v, 0.6:0.3:0.1%w/v, 0.6:0.2:0.2%w/v and 0.6:0.1:0.3%w/v were labelled as batch B1, B2, B3, and B4 respectively. Subsequently, the heated batch of polymer blends and cross-linker calcium chloride ($CaCl_2$, 50mM/L were placed at water bath until the required temperature was reached (37^{O}C). At the desired temperature, the cross-linker was added at four different concentrations (i.e. 3mM/L, 6mM/L, 10mM/L, and 16mM/L) into the emulsion blend with continuous stirring at 250rpm to form hydrogel at 37^{O}C.

Emulsion blend (1ml) and nanovesicle suspension (1ml) were added together with stirring at 250rpm at 42±1^{O}C for 2-5min to homogenously mixed. Subsequently, a pre-defined concentration of $CaCl_2$ (previously heated at the same temperature) was mixed into the emulsion blend containing nanovesicles suspension. Finally, after reaching the desired temperature the solution was poured into 24-well plates at 37^{O}C to set and stored until further analysis. Additionally, hydrogels embedded with rhodamine-6G labeled nanovesicles was prepared for *in-vivo* studies.

2.5. Biopolymeric hydrogel characterization

Hydrogel formulations prepared with preselected concentrations of the cross-linker were subjected to vial tilting method. The technique measures the gelation time at which the solution no longer flowed when the vial was tilted. Macroscopic imaging of pre-formed hydrogels (15mm diameter, 5mm thickness) was studied by visual observation for phase separation and

homogeneity. Cryo-field emission gun-scanning electron microscopy (Cryo-FEG-SEM) was used to accessed the hydrogels morphology using a model of JSM 7600F (at X500 to X15000 magnifications). The pore size of various bare hydrogel formulations was estimated using ImageJ software.

We next performed the rheological characterization by compact modular rheometer of Anton Paar, model Physica MCR 310 and software Rheoplus/32, V3.21 version (Austria) with parallel plate geometry (PP50, diameter 0.27mm, and plate spacing of 1mm). An amplitude sweep study was done at 10Hz frequency with strain varied from 0.01-100% at 37°C to determine the linear viscoelastic region (LVR) of hydrogels formed with different concentrations of cross-linker. The storage (G') and loss (G') modulus indicate elastic and viscous behaviour of materials respectively. This was plotted against oscillatory stress frequency under a constant strain of 0.03% obtained within LVR (previously optimized by strain sweep analysis). Both the modulus (G' and G'') were evaluated at constant strain with varying frequencies sweep from 0.1-10rad/s at 37^0C. Shear-thinning kinetics were studied by measuring the viscosity behaviour of the hydrogels at a shear rate varying from 0.01-100s^{-1} at the physiological temperature of 37^0C.

Furthermore, we conducted the cytocompatibility analysis of the hydrogel by culturing murine fibroblast cells (L929) in the extract of the hydrogels. Gels were sterilized by ^{60}CO irradiation of 20kGy for 48hrs and immerse in Dulbecco's modified eagle medium (DMEM, HiMedia; India). The culture media was supplemented with Fetal bovine serum (10%), antibiotic-antimycotic solution (1%) containing penicillin (10,000U), streptomycin (10mg), and amphotericin-B (25µg) per ml in normal saline (0.9%). Hydrogels at the concentration of 1%w/v in culture media was placed in a humidified atmosphere at 37^0C with 5% CO_2 incubator (IncuSafe, Japan) for 24h. Subsequently, the extracts were collected and filtered them through 0.2µm membrane filter (Millipore) to obtain a test medium. The L929 cells (75-80% confluency) were harvested by treating with 0.25% trypsin-EDTA solution (HiMedia) for 1min. After that, the cells were collected by centrifugation at 1500rpm for 2min and then homogeneously dispersed in culture media. To ensure >95% viability of cells for further experiments we performed dye exclusion assay using trypan blue. The harvested cells were seeded at a density of 5X10^4cell/200µL/well in a 96-well plate and incubated for 24h. After 24h, the exhausted culture medium was exchanged with a fresh culture medium containing different hydrogel extracts in the graded concentrations and incubated for 48hr. After 72hrs,

the exhausted culture median was removed completely and MTT assay was performed to measure the cell viability.

2.6. *In-vivo* release kinetics from hydrogel

TMZ release from different hydrogels embedded with targeted and non-targeted nanovesicles was carried out by the previously described procedure [22] with slight modifications. Concisely, hydrogels with TMZ nanovesicles formulations were immersed into 30ml of simulated cerebrospinal fluid (pH 7.2-7.4) into 50mL tubes and incubated at $37^0 \pm 0.5^0$C at 100±5rpm in the water bath to stimulate *in-vivo* physiological states. To maintained a sink condition, 1mL of media was drawn from the tubes (*n=3*) and replenished with 1mL of fresh media at each predetermined time interval. After 72h, media was changed every day till the completion of the study. The concentration of TMZ existed in the withdrawn aliquots was measured by HPLC analysis using 20µL of injection volume in the C18 column (Jasco, India) at 329nm. The acetonitrile and water containing 0.1% acetic acid (86:14%v/v) was used as mobile phase after appropriate dilutions at 1mL/min flow rate.

Cytotoxicity was carried out with free TMZ and hydrogel embedded with and without TMZ encapsulated nanovesicles on U87MG cells for 72h. Cell viability and IC_{50} were studied by MTT assay and GraphPad prism 5.0 at graded concentrations of TMZ. Transferrin receptors expression on U87MG cells was measured following the previously described method by Yang *et al* using FITC-labelled transferrin (FITC-Tf) binding assay with slight modification [23]. Briefly, $5X10^5$ cells were incubated with FITC-Tf (200µL/mL) at 4°C for 30min. Cells were then washed ice-cold phosphate-buffered saline containing 0.5% bovine serum albumin (BSA). The cells were pelleted down by centrifugation at 1500rpm for 5min and then resuspended in PBS. Cells without treatment (unstained cells) were served as a negative control. FACS calibre flow cytometry analysis was used to measure the cellular fluorescence intensity. Cellular uptake and mechanistic studies in U87MG cells were studied by confocal laser scanning microscopy (CLSM, Olympus Fluoview FV500, Tokyo, Japan) by incubating the hydrogel embedded rhodamine-6G labeled nanovesicles. U87MG cells were grown on glass coverslips and incubated with the different temperature conditions, and endocytosis inhibitors for 1hr. Subsequently, exhausted culture media was replenished with fresh media followed by treatment of cells with hydrogel formulations, and free dye for 2h. Thereafter, excess dye was washed away with ice-cold PBS followed by formalin (10%) fixation of cells on glass slides, and imaged under CLSM. Cytotoxicity was carried out with free TMZ and hydrogel embedded

with and without TMZ encapsulated nanovesicles on U87MG cells for 72h. Cell viability and IC_{50} were studied by MTT assay and GraphPad prism 5.0 at graded concentrations of TMZ.

Additionally, time dependent diffusion of the rhodamine 6G- labeled nanovesicles from the hydrogel matrix was studied using Confocal Laser Scanning microscopy technique.

2.7. *In-vivo* brain uptake and biodistribution studies

Radio-labelling of TMZ loaded nanovesicles was carried out by the previously described method with slight modification [24]. Briefly, non-targeted/targeted nanovesicles (LNs/Tf-LNs-TMZ-40) and the free drug were radio-labeled with technetium by direct tagging using a reducing agent like the aqueous solution of stannous chloride ($SnCl_2$). The 1mg/mL of $SnCl_2$ solution (0.01mL) was mixed with 1mL of test formulation followed by pH adjustment (pH 5-6) using 50mM of sodium bicarbonate buffer. The subsequent mixture was passed through 0.22µm nylon-66 membrane filter. Then the aqueous $^{99m}TcO4$ (2mCi/mL) was added to the filtered mixture and incubated for 15-20min. The factors that affect the maximum labelling efficiency for instance, $SnCl_2$, pH, and incubation time were pre-optimized. Radiolabelling efficiency of the nanovesicles was evaluated by paper chromatography using acetone mobile phase. The paper acting as a stationary phase was cut over and below the mark of test formulation, and region of the solvent front respectively. The gamma counter was used to check the radioactivity on the piece of paper to ensures that the test formulation had labeled with radioactivity. Furthermore, hydrogel (formed with 6mM $CaCl_2$) embedded with TMZ nanovesicles was prepared using the aforementioned radiolabelled procedure (dose: 25mg/kg). Nude mice (male, 25–30g, *n=3*) were treated with 5µL of hydrogel embedded with ^{99m}Tc labeled TMZ targeted and non-targeted nanovesicles (i.e. HG-^{99m}Tc-Tf-LNs-TMZ-40 and HG-^{99m}Tc-LN-TMZ-40 respectively). The 2mCi/mL of ^{99m}Tc was injected intracranially into the mice brain at 2mm right, 1mm posterior to the bregma at a depth of 3mm. Similarly, oral administration of ^{99m}Tc labeled free drug (^{99m}Tc -TMZ) served as a positive control (administered as 250µL by oral gavage). Mice were anesthetized using isoflurane inhalation anaesthesia during an imaging procedure. Blood samples were withdrawn from retro-orbital plexus at 1h, 6h, and 24h following administration to trace the plasma distribution and retention profile of hydrogel embedded with ^{99m}Tc labeled nanovesicles. Furthermore, the radioactivity of ^{99m}Tc labeled formulations in blood and vital organs (heart, brain, lungs, liver, kidney,

bladder, and stomach) was quantified using gamma counter. The results were expressed as the percentage of the dose administered that accumulated in each organ (% ID/cc).

2.8. *In-vivo* intracranial brain tissue penetration and retention study

Intracranial localization of hydrogel embedded with rhodamine-6G (Rh-6G) labeled targeted nanovesicles in tumor-free mice was carried out following the previous method [25] with slight modifications. In brief, a subset of mice was anesthetized using an intraperitoneal 1:1v/v mixture of xylazine and ketamine. On day zero, the skull of mice was drilled and the intracranial cavity was created as described in previous section. Mice were then treated with an intracranial *in-situ* injection of fluorescently labeled 6µL of hydrogel formulation (B3 formed by using 6mM CaCl2) into the cavity using Hamilton® syringe (18G needle). The skull hole was clinched with bone wax followed by suturing and sterilizing the scalp skin by Vet-bond® and povidone-iodine respectively. At 0, 1, and 7 days post hydrogel implantation animals were imaged by a non-invasive IVIS imaging system to confirm localization of formulation within the injected site. After one week, animals were euthanized to isolate the brains. The brain tissue was embedded at optimal cutting temperature (OCT) using the cryo-embedding compound. Consequently, sections of 5µm thickness were fixed on super-frost charged glass slides and maintained at -80°C till further analysis. The brain tissue penetration and retention studies were performed by confocal lesser scanning microscopy to measure the distance from the hydrogel implantation site after nuclei staining with DAPI. Furthermore, we evaluated the potential toxicity of the hydrogel treatment on the brain tissue section of tumor free mice using H and E analysis.

2.9. *In-vivo* evaluation of anti-glioma efficacy of hydrogel

To evaluate the anti-glioma efficacy of hydrogels in orthotopic post-resected GBM induced mouse model intracranial injection of human U87MG cells was performed as described previously [26]. The orthotopic post-operated glioma bearing mouse models we developed exhibited invasiveness, necrosis, and vascular abnormalities due to residual infiltrating tumour cells, which make it a clinically relevant human GBM model of tumour relapse after surgical extraction of primary tumour. In brief, greater than 75% confluent human U87MG cells were trypsinized and washed with Minimum essential medium culture media containing 10% Fetal bovine serum followed by centrifugation for 2min at 1500rpm. The cell pellet was reconstituted in culture media and the cell number was counted by trypan blue for live and dead cell analysis.

The 4.5X10^6 U87MG Luc. live cells were mixed into 3µL sterile phosphate-buffered saline and stereotactically injected into NOD-SCID mice (male, 25–30g) brain at 2mm right, 1mm posterior to the bregma and at a depth of 3mm by creating a burr hole using a microdriller. To clinically mimic the post-resected remnant/residual infiltrating cells that persist in the parenchymal space of the brain after tumour resection, hydrogels treatment was given by *in-situ* injection on the same day itself. Thus, after 5min, the *in-situ* hydrogel formulations (5µl) embedded with targeted/non-targeted nanovesicles were injected using a Hamilton® syringe. The mice were kept undisturbed for 10min to ensure the formation of stable gel followed by superficial sealing of brain hole using sterile bone wax and the skull was closed using Vet-Bond®. Furthermore, tumor-bearing animals were categorized into seven groups (*n=12*/group) such as untreated control (cavity with U87MG Luc. cells), bare hydrogel (hydrogel without nanovesicles), hydrogel embedded with TMZ loaded targeted (HG-Tf-LNs-TMZ-40), and non-targeted (HG-LNs-TMZ-40) nanovesicles at the dose of 25mg/kg (previously optimized), and hydrogel embedded with targeted and non-targeted nanovesicles without TMZ (HG-Tf-LNs-40, HG-LNs-40). The positive control group received a similar dose of TMZ by oral route. Animals were examined for tumour development by non-invasive bioluminescence imaging scan at pre-determined time intervals. Mice were regularly monitored for body weight and general health status. Mice showing massive tumour burden with grade-4 symptoms were euthanized by cervical dislocation followed by isolation of brain tissue for histopathological analysis. For anti-glioma efficacy study, the tumour growth was calculated by bioluminescence scan performed as the function of the signal generated by photon due to catalysis of luciferin which was injected 2min before the imaging. The tumour burden was expressed as total flux (photon/second) versus days. Furthermore, mice were monitored for body weight, and neurological deficit scale scoring was used to score the clinical signs such as grade-0: healthy, grade-I: mild one-sided paralysis, grade-2: moderate one-sided paralysis, and/or hunchback beginning, grade-3: severe one-sided/both-sided paralysis, and prominent hunchback, and grade-4: dying mice. Previous studies had shown tumour invasion wherein tumour cells were spread along with the perivascular space in areas adjacent to the tumour mass. Tumour cells was also found to invade along with the subpial space with tracking along with Virchow-Robin spaces back into the brain. Thus, overall findings suggest the areas of necrosis and viable diffuse infiltrative glioma as the end-points for pathological correlation in mice and humans. Animals were kept in sterile conditions having free access to normal food and water to avoid any type of stress. Similarly, we performed the gross imaging and tumor volume **[34]**

measurement of the isolated tumor brain tissues of the mice treated with different treatment groups. For histopathological study, poly-L-lysine-coated slides were with 4µm of tissue section used for formalin fixation and paraffin-embedding. Uncoated slides were used for haematoxylin-eosin (H and E) staining analysis. Additionally, for immunohistochemistry tumour sections were deparaffinized using xylene and stained as per the manufacturer's protocol for the Ki67 antibody. Four random areas were acquired in each section and analysed for Ki67 proliferation index (%) by counting Ki67 positive tumour cells to total no. of tumour cells using bright-field microscopy. Furthermore, immunohistochemistry staining of Caspase-3 apoptosis marker analysis in the brain tissue of the post-surgically treated orthotopic GBM bearing mice was studied by bright filed microscopy to evaluate the proapoptotic effect of miltifosine with TMZ.

2.10 Ethical statement for animal studies

Animals were maintained in the laboratory animal facility of ACTREC following the national guidelines mentioned by **the Committee for the Purpose of Control and Supervision of the Experiments on Animals (CPCSEA)**, Ministry of Fisheries, animal Husbandry and Dairying department of animal Husbandry and Dairying, Government of India. The *Institutional Animal Ethics Committee* (IAEC) of the Advanced Centre for Treatment Research and Education in Cancer (ACTREC), Tata Memorial Centre, India, Registration no. 65/GO/ReBiBt/S/99/CPCSEA approved the protocol (**IAEC protocol no. 07/2017**). The animal studies were performed only after taking prior consent and approval from the Institutional Animal Ethics Committee, ACTREC. All the experiments were conducted in strict accordance for the care and use of the laboratory animals. A controlled environment was provided to the animals with a temperature of 22±2°C and relative humidity maintained at 40-70%. A 12 hours' day night cycle was maintained (7:00 to 19:00 day and 19:00 to 7:00 night). The animals were given gamma irradiated balanced diet (Altromin 1314P) and sterile water. Individually ventilated Cage system (IVC, M/S Citizen, India) was used to house mice. These IVCs were provided with autoclaved corn cob as bedding for the mice. Animal euthanasia was done under the supervision of attending veterinarian using CPCSEA recommended euthanizing agent, carbon dioxide.

Supplementary data

3. Results

3.1. Engineering of temozolomide-miltefosine encapsulated nanovesicles

Optimized formulation of TMZ loaded non-targeted nanovesicles had hydrodynamic diameter of 118±4nm. The chosen phospholipid mixture was composed of soya phosphatidylcholine (SPC), and hexadecyl phosphocholine (HePc) or miltefosine (3:2mol%) and 1,2-dioleoyl-sn-glycero-3-phosphoethanolamine (DOPE served as linker lipid with 1/10th weight of total lipid). Although all the non-targeted nanovesicles with TMZ had shown negative zeta potential values but the maximum negative zeta potential of -30±0.7mV was observed for LNs-TMZ-40 as compared to other non-targeted nanovesicles (Fig.**S1a**). SPC and HePc were chosen to impart chemical stability and synergistic proapoptotic activity to the prodrug TMZ encapsulated in the nanovesicle. The average encapsulation efficiency of TMZ was found to be 90±7.0% (Fig.**S1b**). The optimal coupling efficiency of Tf was 995.6±76.8µg/µmole of phospholipids with nanovesicles. The zero length carbodiimides crosslinker namely 1-ethyl-3-[3-dimethylaminopropyl] carbodiimide (EDC) was used for Tf conjugation under acidic conditions (pH 6) using MES buffer. After Tf modification, particle size and surface charge of preselected nanovesicles increased to 228±6nm and -40±0.6mV, respectively (Fig.**S1h**). Similar finding was observed with blank nanovesicle before and after Tf coupling (Fig.**S2a,b**). Furthermore, flow cytometry measurement showed the shift of fluorescein ($A_1 \rightarrow C_1$) and Nile red ($B_1 \rightarrow D_1$) intensity for targeted nanovesicles (D) in comparison to unstained targeted nanovesicles (A) thereby confirming the coupling of Tf on the nanovesicles surface (Fig. **S1i**).

Supplementary figures

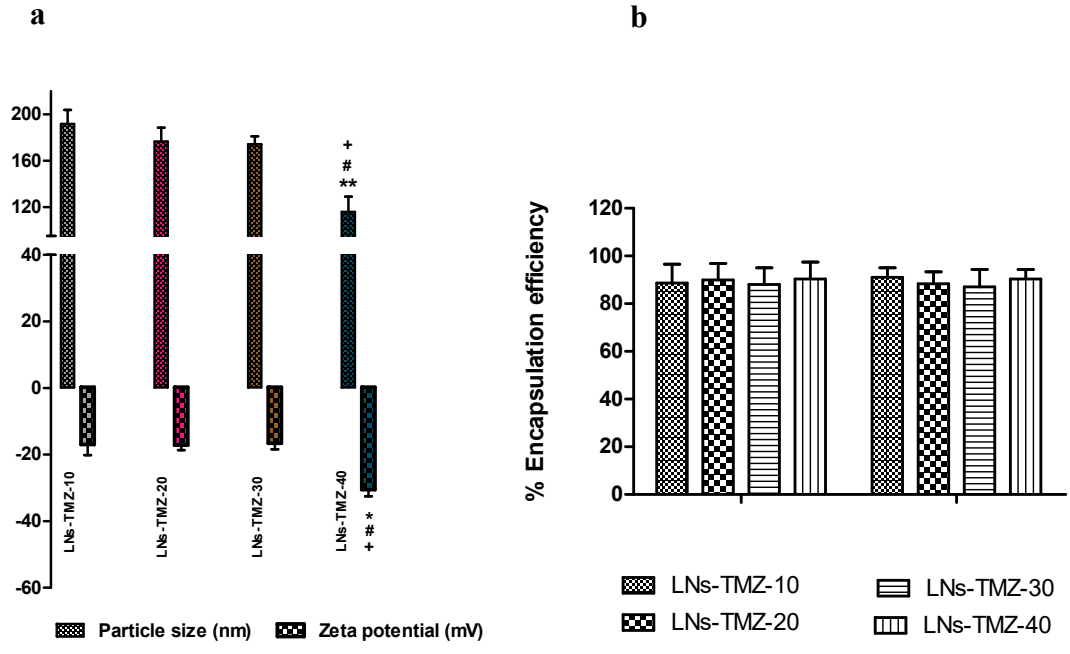

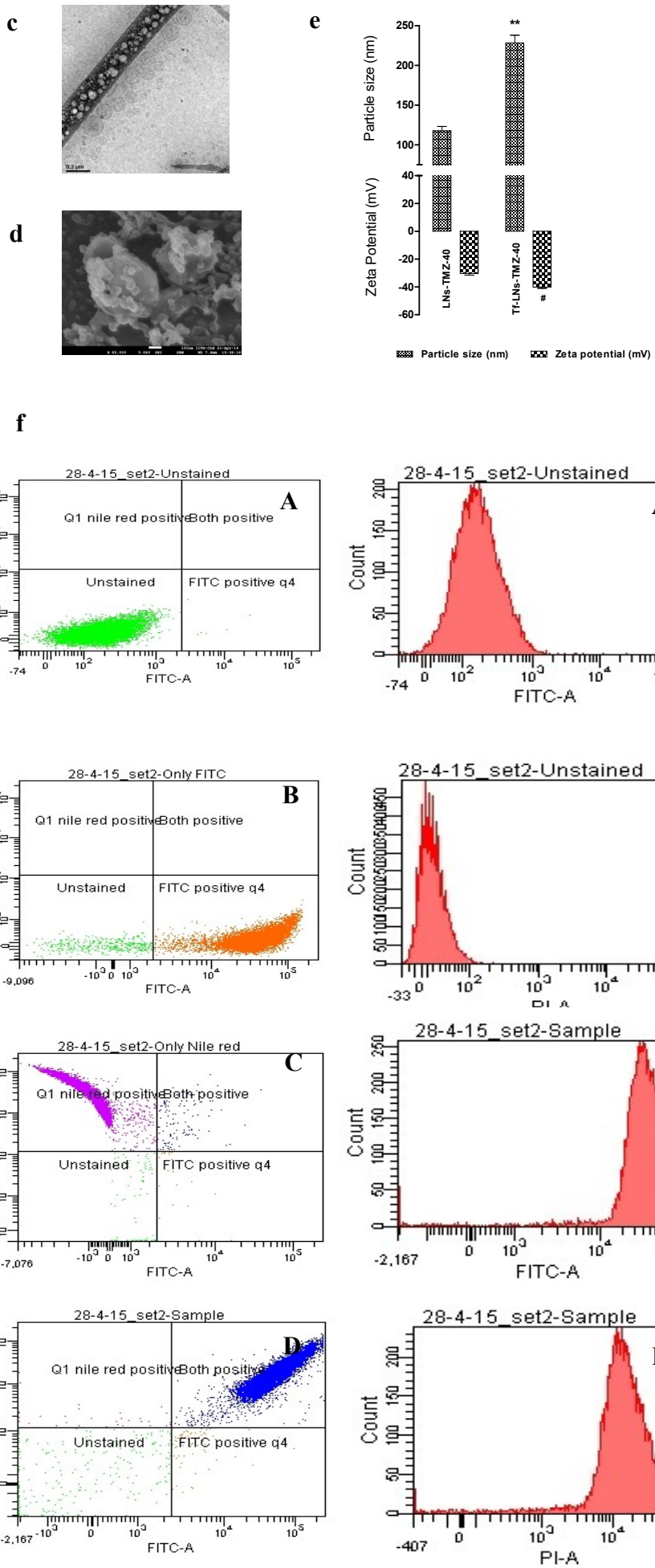
c
d
e
Particle size (nm)
Zeta Potential (mV)
LNs-TMZ-40
Tf-LNs-TMZ-40
**
#
Particle size (nm)
Zeta potential (mV)
f
28-4-15_set2-Unstained
A
Q1 nile red positive
Both positive
Unstained
FITC positive q4
PI-A
FITC-A
28-4-15_set2-Unstained
A1
Count
FITC-A
28-4-15_set2-Only FITC
B
28-4-15_set2-Unstained
B1
28-4-15_set2-Only Nile red
C
28-4-15_set2-Sample
C1
28-4-15_set2-Sample
D
28-4-15_set2-Sample
D1

Fig S1. **Characterization of postoperative flexible targeted particle in gel for GBM treatment** (**a**) Graphical presentation of particle size analysis of TMZ loaded nanovesicles. Results presented as mean±SEM, showing significant difference at $^{**}p\leq0.01$ for LNs-TMZ-40 *vs.* LNs-TMZ-10 and $^{\#,+}p\leq0.05$ for LNs-TMZ-40 *vs.* LNs-TMZ-20 and LNs-TMZ-30 for size analysis study and $^{*}p\leq0.05$ for LNs-TMZ-40 *vs.* LNs-TMZ-10, $^{\#}p\leq0.05$ for LNs-TMZ-40 *vs.* LNs-TMZ-20, $^{+}p\leq0.05$ for LNs-TMZ-40 *vs.* LNs-TMZ-30, for surface charge analysis study *(n=3)*. **(b)** Graphical representation of encapsulation efficiency of TMZ loaded nanovesicles before and after Tf targeting performed by LC-MS/MS technique. Values were expressed as mean±SEM showing statistically non-significant difference at $^{ns}p\geq0.05$, *(n=3)* and representative images by **(c)** high resolution-cryo-transmission electron microscopy of TMZ nanovesicles before targeting (scale bar: 200nm), **(d)** cryo-field emission gun scanning electron microscopy of TMZ nanovesicles after Tf targeting (scale bar: 100nm) (**e**) particle size, and zeta potential of TMZ encapsulated nanovesicles before and after Tf targeting expressed as mean±SEM, showing significant difference at $^{**}p\leq0.01$ for Tf-LNs-TMZ-40 *vs.* LNs-TMZ-40 and $^{\#}p\leq0.05$ for Tf-LNs-TMZ-40 *vs.* LNs-TMZ-40 respectively, (n=3), (**f**) flow cytometry measurement showing (A-D) density plot and (A_1-D_1) histogram of (A) targeted particles unstained (control) (B) only FITC labelled targeted particles (C) only Nile red labelled targeted particles and (D) targeted particles with both the dyes.

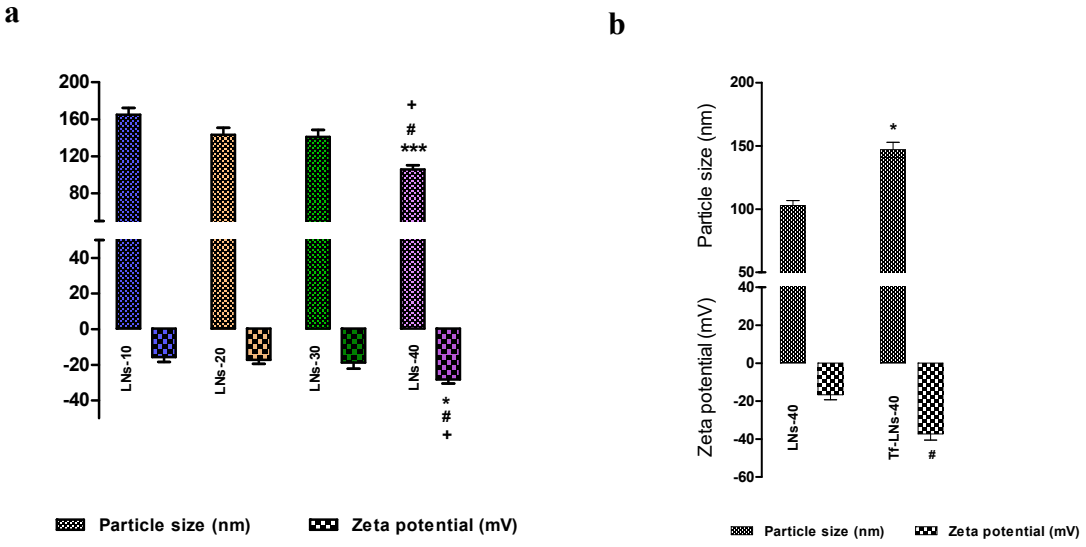

Fig S2. **Characterization of lipid nanovesicles without temozolomide**. (**a**) Particle size of lipid nanovesilces presented as mean ± SEM, showing significant difference at $^{***}p\leq0.001$ for LNs-40 *vs.* LNs-10 and $^{\#,+}p\leq0.05$ for LNs-40 *vs.* LNs-20 and LNs-30 and $^{*,\#,+}p\leq0.05$ for LNs-40 *vs.* LNs-10, LNs-20, LNs-30, for surface charge analysis study *(n=3)*, (**b**) particle size of optimized lipid nanovesicles before (LNs-40) and after (Tf-LNs-40) transferrin targeting, showing significant difference at $^{*,\#}p\leq0.05$ for Tf-LNs-40 *vs.* LNs-40 for size and surface charge analysis studies, (n=3)

a

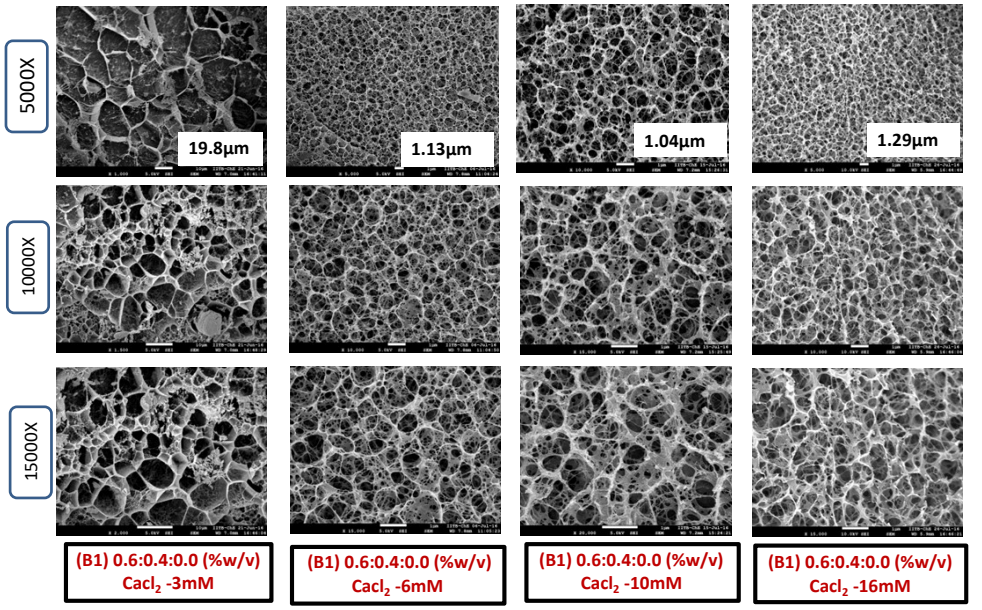
5000X
10000X
15000X
19.8µm
1.13µm
1.04µm
1.29µm
(B1) 0.6:0.4:0.0 (%w/v) Cacl2 -3mM
(B1) 0.6:0.4:0.0 (%w/v) Cacl2 -6mM
(B1) 0.6:0.4:0.0 (%w/v) Cacl2 -10mM
(B1) 0.6:0.4:0.0 (%w/v) Cacl2 -16mM

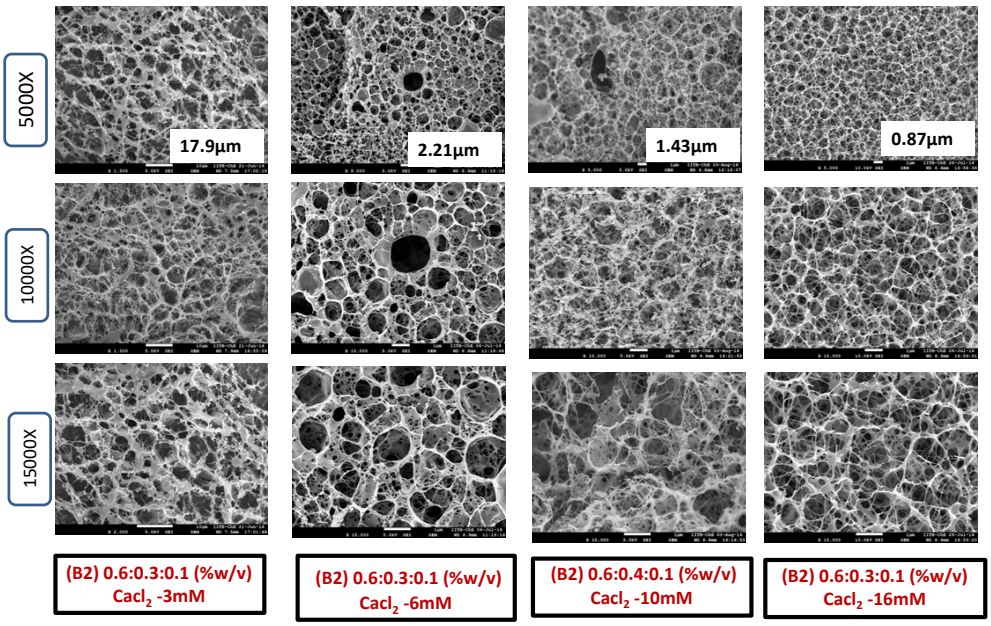
5000X
10000X
15000X
17.9µm
2.21µm
1.43µm
0.87µm
(B2) 0.6:0.3:0.1 (%w/v) Cacl2 -3mM
(B2) 0.6:0.3:0.1 (%w/v) Cacl2 -6mM
(B2) 0.6:0.4:0.1 (%w/v) Cacl2 -10mM
(B2) 0.6:0.3:0.1 (%w/v) Cacl2 -16mM

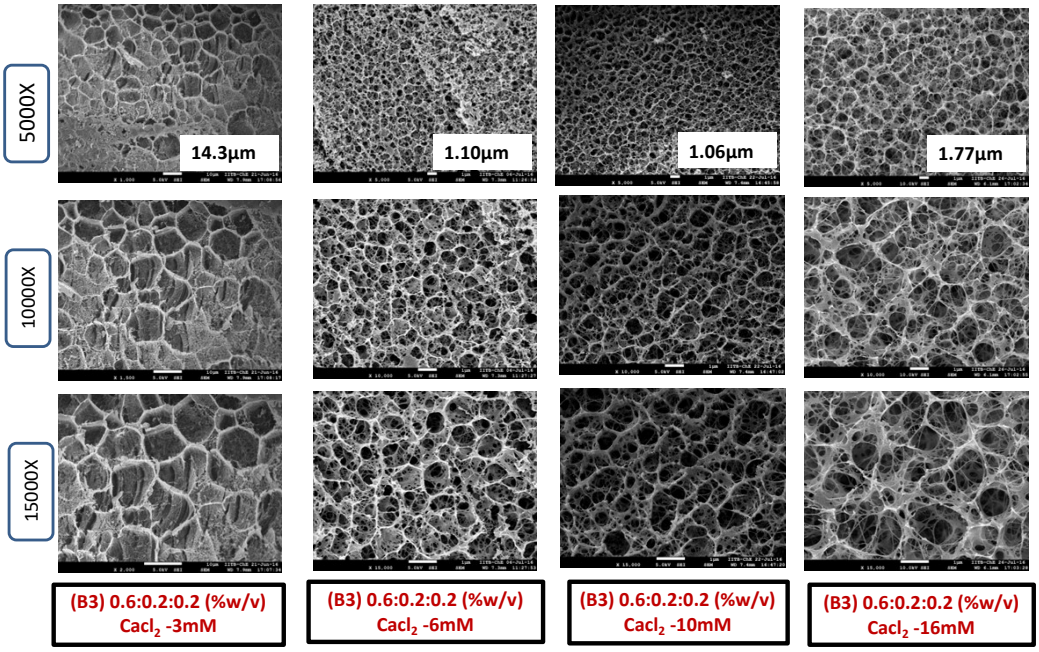
5000X
10000X
15000X
14.3µm
1.10µm
1.06µm
1.77µm
(B3) 0.6:0.2:0.2 (%w/v) Cacl2 -3mM
(B3) 0.6:0.2:0.2 (%w/v) Cacl2 -6mM
(B3) 0.6:0.2:0.2 (%w/v) Cacl2 -10mM
(B3) 0.6:0.2:0.2 (%w/v) Cacl2 -16mM

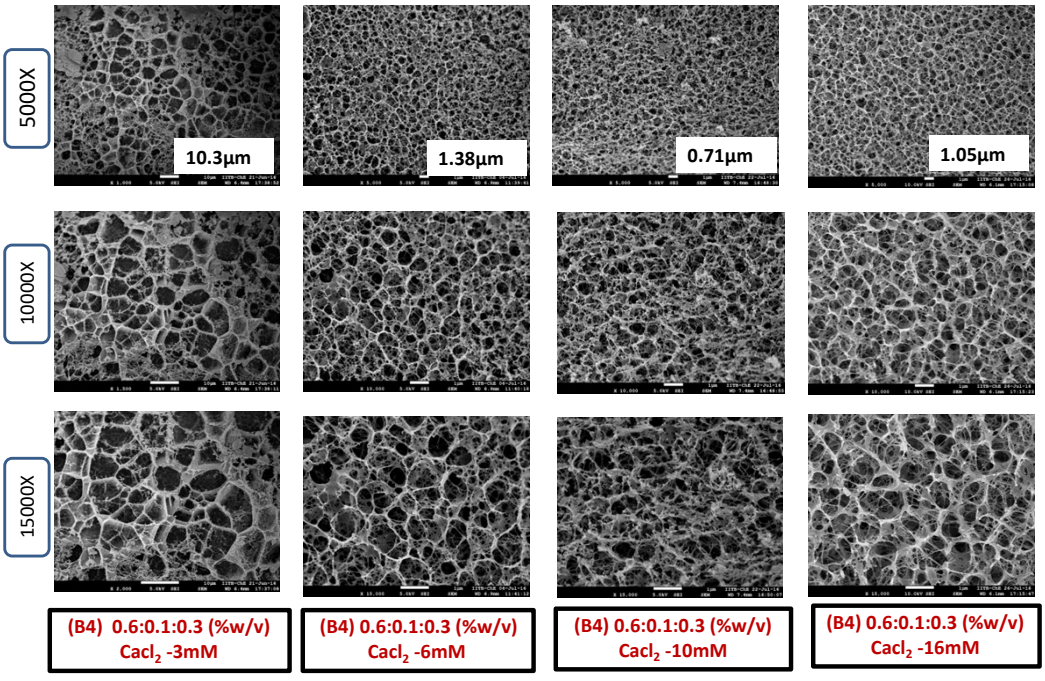
5000X
10000X
15000X
10.3µm
1.38µm
0.71µm
1.05µm
(B4) 0.6:0.1:0.3 (%w/v) Cacl2 -3mM
(B4) 0.6:0.1:0.3 (%w/v) Cacl2 -6mM
(B4) 0.6:0.1:0.3 (%w/v) Cacl2 -10mM
(B4) 0.6:0.1:0.3 (%w/v) Cacl2 -16mM

b

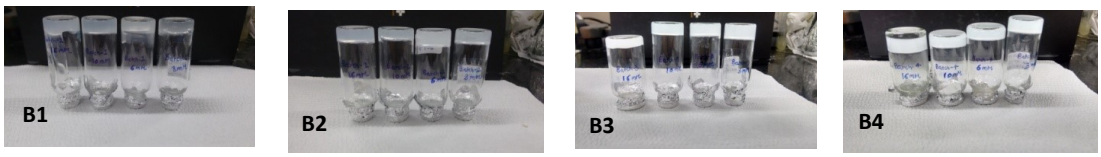
B1
B2
B3
B4

c

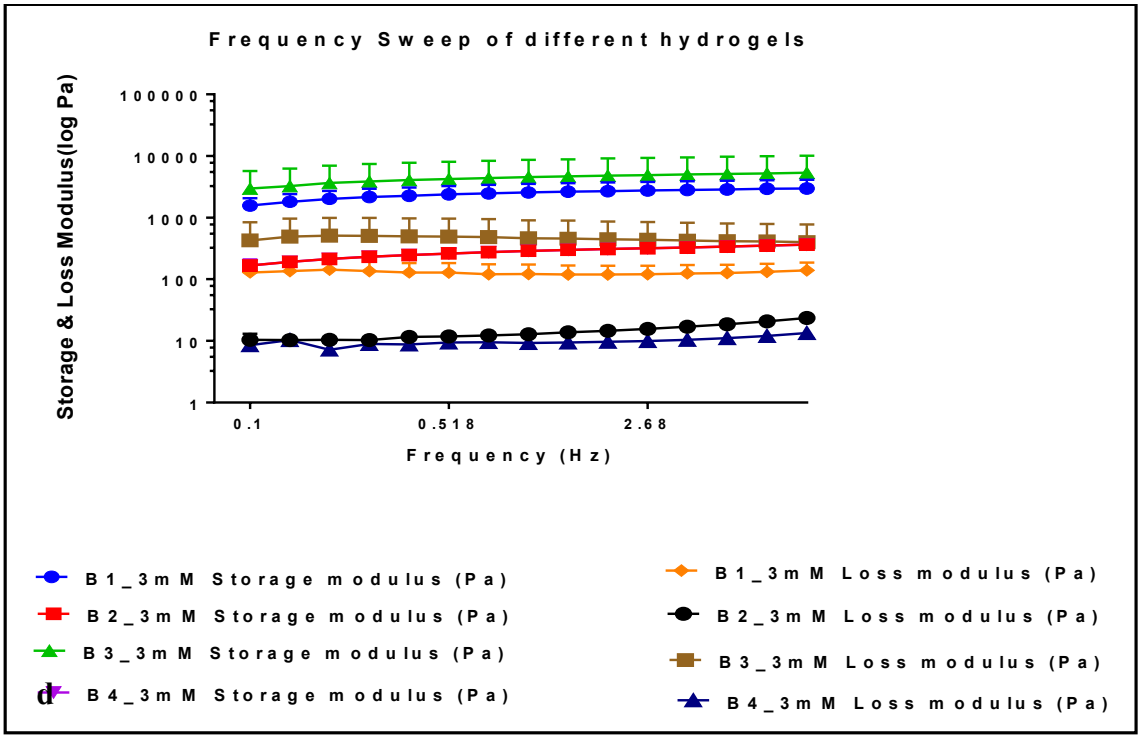
Frequency Sweep of different hydrogels
Storage & Loss Modulus(log Pa)
100000
10000
1000
100
10
1
0.1
0.518
2.68
Frequency (Hz)
B1_3mM Storage modulus (Pa)
B2_3mM Storage modulus (Pa)
B3_3mM Storage modulus (Pa)
B4_3mM Storage modulus (Pa)
B1_3mM Loss modulus (Pa)
B2_3mM Loss modulus (Pa)
B3_3mM Loss modulus (Pa)
B4_3mM Loss modulus (Pa)

d

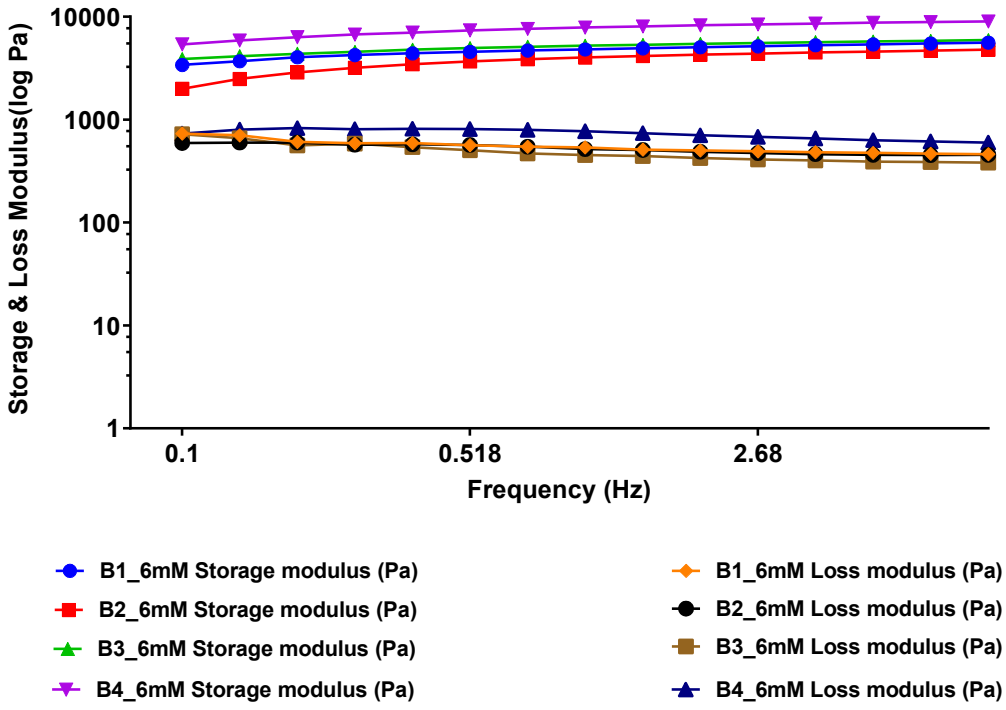
Storage & Loss Modulus(log Pa)
10000
1000
100
10
1
0.1
0.518
2.68
Frequency (Hz)
B1_6mM Storage modulus (Pa)
B2_6mM Storage modulus (Pa)
B3_6mM Storage modulus (Pa)
B4_6mM Storage modulus (Pa)
B1_6mM Loss modulus (Pa)
B2_6mM Loss modulus (Pa)
B3_6mM Loss modulus (Pa)
B4_6mM Loss modulus (Pa)

e

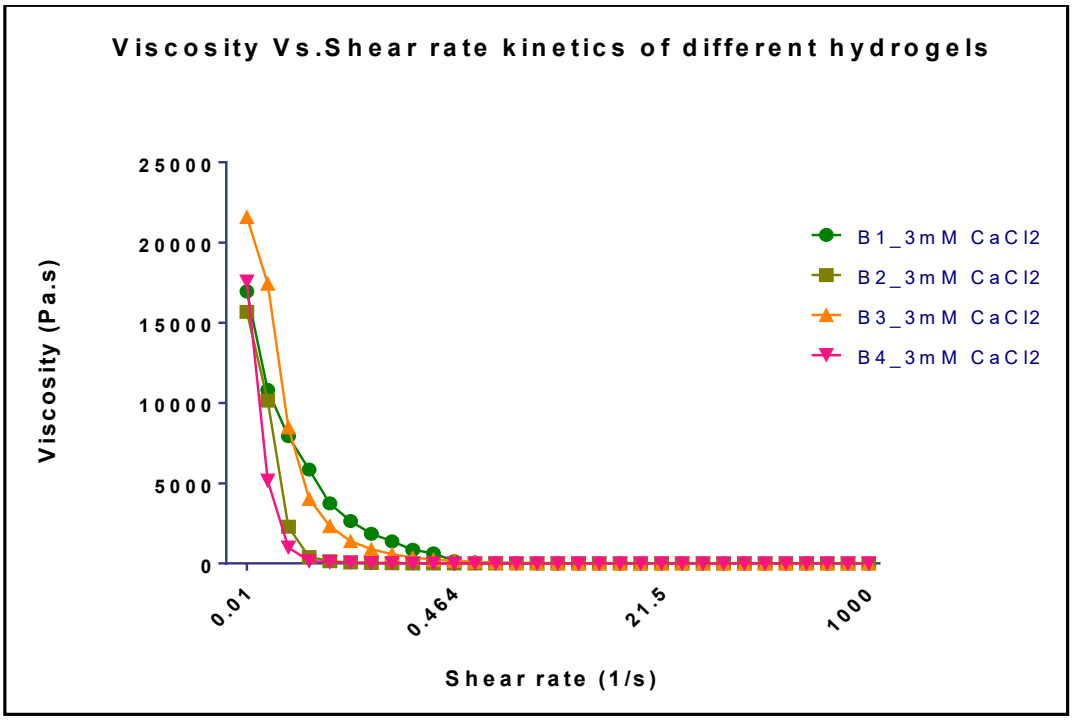

f

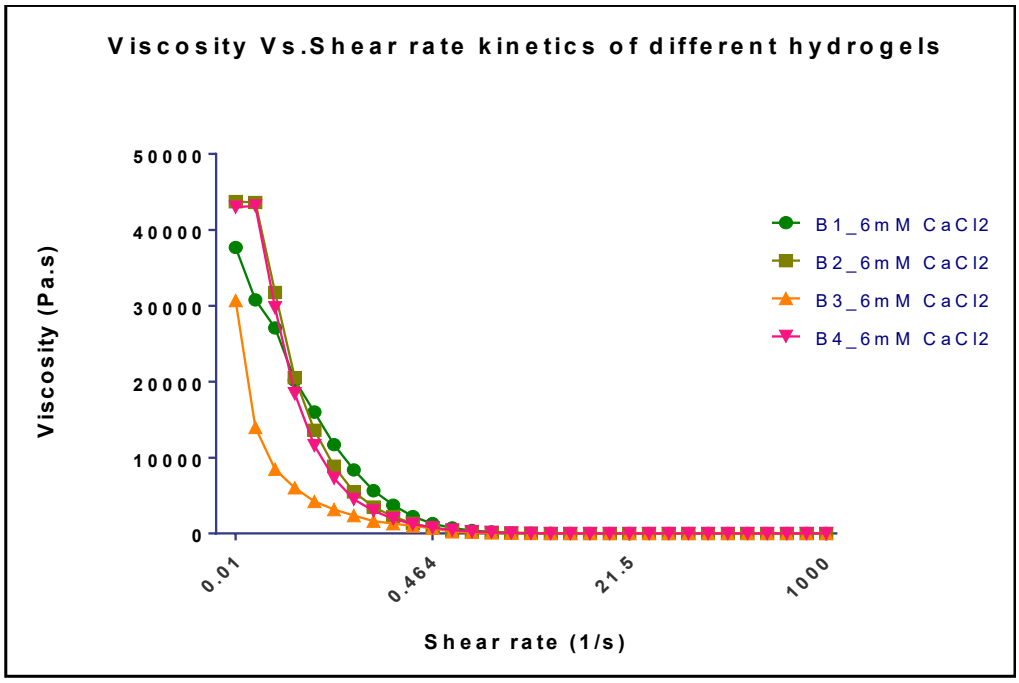

Fig S3. Gelation kinetics and rheological characterization of implantable hydrogels. (a) cryo-field emission gun-scanning electron microscopy images of all hydrogels (HGs: B1 B2,

B3 and B4) formed by 3mM, 6mM, 10mM and 16mM conc. of $CaCl_2$ [Scale bar: 1µm, under X5000, X10000 & X15000 magnifications] **(b)** determination of gelation time at 37^{O}C of all HGs formulations by inverted glass vial method. **(c,d)** comparative evaluation of storage modulus (G′) verses loss modulus (G″) of optimized hydrogels prepared 3mM and 6mM concentration of crosslinker using frequency sweep measurement. Values were presented as mean ± SEM. One-way ANOVA indicating significant difference at $^{****}p\leq0.0001$, $^{***}p\leq0.001$and $^{**}p\leq0.01$, $^{*}p\leq0.1$ and $^{ns}p\leq0.5$. **(e,f)** comparative evaluation of viscosity verses shear rate profile of optimized hydrogels cross-linked with 3mM and 6mM concentration of crosslinker, showing shear thinning behaviour. Values were presented as mean ± SEM. One-way ANOVA indicating significant difference at $^{****}p\leq0.0001$, $^{***}p\leq0.001$ and $^{**}p\leq0.01$, $^{*}p\leq0.1$ and $^{ns}p\leq0.5$, $(n=3)$.

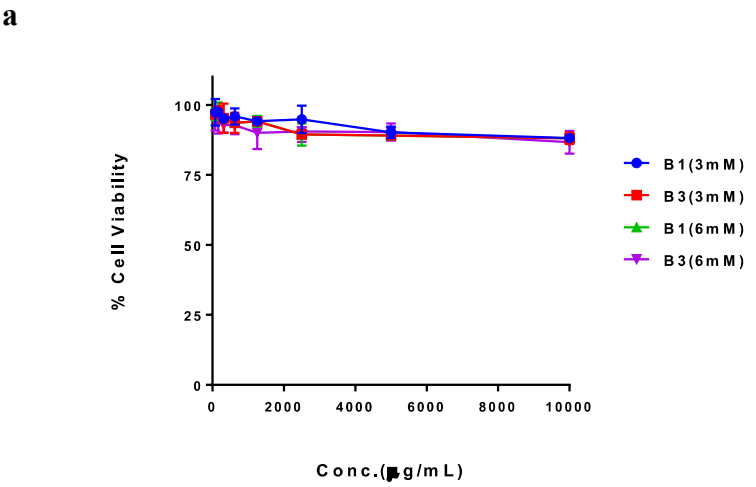

Fig. S4. *In-vitro* cytocompatibility of various hydrogels at different concentrations on murine fibroblast cells after 72hr post-treatment using MTT assay. Values were presented as mean ± SEM, (*n=3*).

Table S1. Gelation time for gellan/HPMC and gellan/HPMC/PCL after addition of $CaCl_2$.

Composition GG: HPMC: PCL (%w/v)	**Temp. (°C)**	**Rotation per minute (RPM)**	**Gelation time (min) at 37°C w.r.t conc. of $CaCl_2$**			
			3mM	**6mM**	**10mM**	**16mM**
B1- 0.6:0.4:0.0	48-50	200	16±3	9±2	7±3	3±2
B2- 0.6:0.3:0.1	45-50	200	14±2	7±3	6±2	2±1

B3- 0.6:0.2:0.2	45-50	200	13±2	6±2	3±1	1±1
B4- 0.6:0.1:0.3	45-50	200	10±2	5±1	2±1	1±1

Table S2. *In-vivo* anti-glioma efficacy of different hydrogel formulations using Kaplan Meier survival analysis on orthotopic post-resection GBM induced mouse model.

Treatment group	Median survival (days)	Tumor free survival
Control (cavity with cells)	33±2	No
Bare hydrogel (HG)	32±3	No
HG-LNs-40	62±2	No
HG-Tf-LNs-40	72±4	No
HG-LNs-TMZ-40	110±2	50%
HG-Tf-LNs-TMZ-40	130±2	50%